Speed Estimation in Geared Wind Turbines Using the Maximum Correlation Coefficient

Georgios Alexandros Skrimpas[1], Kun S. Marhadi[2], Bogi Bech Jensen[3], Christian Walsted Sweeney[4], Nenad Mijatovic[5], and Joachim Holboell[6]

[1,2,4] *Brüel and Kjær Vibro, Nærum, 2850, Denmark*
alexandros.skrimpas@bkvibro.com
kun.marhadi@bkvibro.com
christian.sweeney@bkvibro.com

[3] *University of the Faroe Islands, Tórshavn, 100, Faroe Islands*
bogibj@setur.fo

[5,6] *Technical University of Denmark, Lyngby, 2800, Denmark*
nm@elektro.dtu.dk
jh@elektro.dtu.dk

ABSTRACT

Valid speed signal is essential for proper condition monitoring of modern variable speed wind turbines. Traditionally, a tachometer mounted on the high speed shaft provides reference for tracking speed dependant frequency components, such as generator speed harmonics and gearbox tooth mesh frequencies. The health assessment of drive train components is limited to broadband measurements when the speed signal is invalid. This condition results in reduced fault detection capabilities and consequently decreased lead time. In this work, a new speed estimation algorithm is presented in order to overcome the above mentioned issues. The high speed stage shaft angular velocity is calculated based on the maximum correlation coefficient between the 1^{st} gear mesh frequency of the last gearbox stage and a pure sinus tone of known frequency and phase. The proposed algorithm utilizes vibration signals from two accelerometers for cross-referencing purposes. The method is tested in three drive train configurations, where 720 sets of vibration signals of $10.24s$ length, sampled at $25.6kHz$ are analysed. Consistent speed estimation reaches approximately 98% when two vibration sources are utilized, whereas it is lower when only one source is taken into account. No apparent patterns arise between speed variation levels or power production and the number of invalid outputs, showing the independence of the method from operational parameters.

1. INTRODUCTION

Condition monitoring of wind turbine drive trains can be considered as a procedure carried out in two layers (Andersson, Gutt, & Hastings, 2007). In the first layer, extracted condition indicators (CI), corresponding to characteristic frequencies describing the state of a component, are employed for long time trending and alarming. Gearbox tooth mesh frequencies (Bartelmus & Zimroz, 2009; Taylor, 2000), energy in the high or low frequency range (Marhadi & Hilmisson, 2013) and running speed harmonics (Wu, Lin, Han, & Ding, 2009) are typical CIs used by condition monitoring experts. The diagnostic process is moved to the second layer when an alarm is generated, where detailed analyses in time and frequency domains take place in order to verify the presence and nature and consequently assess the severity of a developing fault.

The above described condition monitoring scheme relies on the capability of generating alarms based on both speed and not-speed related condition descriptors. If the generator speed signal is invalid, due to either hardware problem or improper installation, monitoring of the drive train components is limited to broadband measurements, which provide vague information regarding the nature of the fault. Hence, failure modes manifested as developing speed related frequencies, such as the second running speed harmonic in case of misalignment between the generator and gearbox, are challenging to be detected in early stage resulting in reduced lead time for inspection and correction

Several speed estimation techniques have been developed and

proposed the past few years utilizing vibration signals such as resampling in the angular domain (Bonnardot, Badaloui, Randall, Danie're, & Guillet, 2005; Villa, Reñones, Perán, & De Miguel, 2011; Urbanek, Zimroz, Barszcz, & Antoni, n.d.), Chirplet transform (Peng et al., 2011), combination of Chirplet transform and Vold-Kalman filtering (Zhao, Lin, Wang, Lei, & Cao, 2013), short–time scale transformation (Combet & Zimroz;, 2009), methods in the time–frequency domain (Zimroz, Millioz, Martin, et al., 2010; Zimroz et al., 2011) and harmonic decomposition (Yiakopoulos, Gryllias, & Antoniadis, 2009). Furthermore, tacholess approaches are adopted in order to mitigate the reduction in effectiveness of the speed sensor in variable speed conditions (Borghesani, Pennacchi, Randall, & Ricci, 2012; Coats, Sawalhi, & Randall, 2009).

The present paper investigates the feasibility of extracting the speed signal by tracking a running speed multiple in the time domain, such as the mesh frequency of the gearbox high speed stage. The method is based on locating the maximum correlation coefficient between the selected spectral component and a pure sinus tone. This technique constitutes an effort to utilize the raw vibration signal while decoupling the estimation of the instantaneous frequency from the frequency and angular domains.

The paper is organised as follows. The mathematical background of the maximum correlation coefficient method is presented in section 2. The challenges regarding the speed estimation process in general are discussed in section 3 . Section 4 presents the developed algorithm utilizing two vibration sources. The validation of the method is tested offline in 120 turbines of three different drive train topologies and the results are shown in section 5. Finally, the main conclusions are discussed in section 6.

2. USE OF MAXIMUM CORRELATION COEFFICIENT FOR FREQUENCY ESTIMATION

2.1. Method Description

The extraction of frequency f_a, within a predefined range $[f_{low}, f_{high}]$, and angle ϕ_a, where $\phi_a \in (-\pi/2, \pi/2]$, of a signal $x_a(n)$, where n is the sample number, sampled at F_s can be achieved in the time domain via the maximum correlation coefficient method (MCC) (Bellini, Franceschini, & Tassoni, 2006). Based on this technique, a test signal $x_b(n,k,l)$ of frequency $f_b(k)$ and phase $\phi_b(l)$ sampled at F_s is generated and the correlation coefficient $C_{a,b}(k,l)$ between the two signals $x_a(n)$ and $x_b(n,k,l)$ is calculated. The values of $f_b(k)$ and $\phi_b(l)$ which yield the highest absolute correlation coefficient $C_{a,b}(k,l)$ provide the estimation of the initial signal frequency f_a and angle ϕ_a respectively.

$$x_b(n,k,l) = A_b sin\left(\frac{2\pi f_b(k) n}{F_s} + \phi_b(l)\right) \tag{1}$$

where $f_b(k) \in [f_{low}, f_{high}]$ and $\phi_b(l) \in (-\pi/2, \pi/2]$. Parameters k and l refer to the frequency and phase difference between two consecutive test frequencies and angles respectively and they depend on the desired accuracy.

$$C_{a,b}(k,l) = \frac{cov(x_a(n), x_b(n,k,l))}{\sqrt{cov(x_a(n), x_a(n)) \cdot cov(x_b(n,k,l), x_b(n,k,l))}} \tag{2}$$

$$f_a \approx f_b(k) \;\; and \;\; \phi_a \approx \phi_b(l) \;\; for \;\; k,\; l \mid |C_{a,b}(k,l)| = max \tag{3}$$

The approximation sign is used in order to denote that the calculated quantities are approximations of the true values depending on the specified resolution.

Figure 1 illustrates the signal described in equation 4 of total length equal to 0.5 seconds, which consists of a strong sinusoidal tone of $20Hz$ and initial phase 60^o, a weaker signal at $8Hz$ and white Gaussian noise ν. The objective is to estimate the dominant frequency and corresponding phase within this short time interval.

$$x_a(n) = sin\left(2\pi 10n + 60^o\right) + 0.4sin\left(2\pi 4n\right) + \nu \tag{4}$$

Assuming that a rough estimation of the frequency band is available ($[f_a - f_{range}, f_a + f_{range}]$[1]), and selecting the frequency and phase resolutions to be $0.05Hz$ and 9 degrees respectively, the calculated test frequency and phase are

$$f_b = 20Hz \;\; and \;\; \phi_b = 61.6^o \tag{5}$$

Figure 2 shows a contour plot of the absolute correlation coefficient as function of the test frequencies and phases. There are two sets of maxima, for the two components of $x_a(n)$, i.e. $8Hz$ and $20Hz$. The optimum value is indicated by a data cursor, corresponding to frequency and phase of $20Hz$ and 61.6^o; the maximum correlation coefficient value is 0.9242. The maximum tracked frequency is moderately dependant on phase, varying approximately 3.5% from the true value at angle approximately minus 90^o off the actual phase.

In the following time section, e.g. next 0.5 seconds, the same process would be repeated and the proper frequency estimation is yielded if the the frequency of interest alters. In wind turbine applications, the expected frequency is assessed to be close to the former result, hence making the process faster by keeping a small frequency range of search.

The maximum correlation coefficient method does not pro-

[1]The parameter f_{range} is highly dependent on the validity of the provided information and influences directly the computational cost of the method.

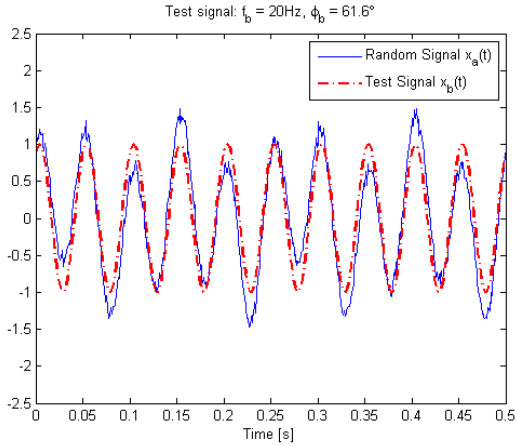

Figure 1. Random signal (blue line) and test signal (dashed red line) of frequency $f_b = f_a$.

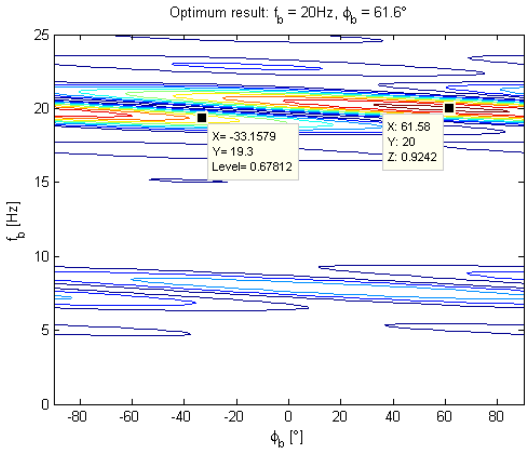

Figure 2. Surface plot of the absolute correlation coefficient as function of frequency f_b and phase ϕ_b. The optimum and worse results are marked by two data cursors. The frequency step is $0.05Hz$ and the phase step is 9^o.

vide full frequency representation of the initial signal $x_a(t)$, but it is limited on tracking a specific spectral component. The provided information is not restricted to the frequency of the selected spectral component, but reliable phase angle can be also calculated with the cost of increased computational needs. The drawback of the maximum correlation coefficient method lays on the lack of information regarding the amplitude of any frequency component. However, the amplitude is not crucial in the frame of feeding a reference speed to the condition monitoring system and thus the robustness and consistency are not affected. The method is capable of yielding accurate results in short time intervals, e.g. 0.3 seconds, under the assumption of constant speed, whereas in the frequency domain the corresponding resolution is 3.33 Hz, which is considered poor.

3. SPEED ESTIMATION CHALLENGES

The commonest location of vibration signals utilized for speed reconstruction is on the gearbox high speed stage, mainly due to the high energy content of the generated vibrations. However, numerous factors may complicate the process and jeopardize the accuracy of speed estimation. Some of the major challenges are listed below.

1. initial selection of the search bandwidth of the frequency of interest
2. identification of a known suitable speed related frequency, which is adequately represented within the available time interval and is dominant in the aforementioned frequency range
3. verification of results and redundancy in case of invalid signal dynamics of the selected accelerometers
4. guarantee of consistent results regardless the operating condition

The first three points are discussed in the following subsections, whereas the fifth is discussed in section 5, where the results are presented.

3.1. Selection of initial search frequency range

The core of speed estimation based on the maximum correlation coefficient method is the selection of the initial search range. If the frequency of interest is not within the specified bandwidth, the method yields invalid results introducing high uncertainty in the fault diagnosis procedure.

So, it is essential to select a relatively broad frequency range for the running speed regardless the operating conditions. A parameter which could assist on the bandwidth selection and is simultaneously available in all wind turbines is the instantaneous power production. Of course, this approach shall not be applied globally, but fine tuning is suggested for all gearbox types and ratios.

Figure 3 illustrates the mean running speed of approximately 70000 10.24 seconds files as function of the active power production from approximately 500 $3.0MW$ geared wind turbines with a gearbox ratio close to $1 : 110$, operating from 2009 to present. In order to ensure that the power generation is relatively constant within the above mentioned time length, the condition that the speed variation of the acquired file is less than $1Hz$ has to be met in the present application. Furthermore, any power values above $3.3MW$ are neglected, so the cases where the turbine controller parameters are invalid, do not affect the distribution. The same applies for the recorded generator speeds over $35Hz$.

A wide range of running speed values applies for the same power production, fact which complicates the selection of the initial bandwidth. The latter must include all potential cases

on one hand, but on the other hand a valid calculation has to be executed within the specified computational time.

If a wide dynamic range is considered for the initial estimation of the running speed, as shown in Figure 3 with green circles, then it can be guaranteed that the actual rotational speed is within this band rendering the method independent of any special considerations for each wind park or turbine. It can be observed in Figure 3 that by following the above described concept for the estimation of the initial speed, the number of outliers on the low power bins is minimized while keeping an acceptably low frequency band.

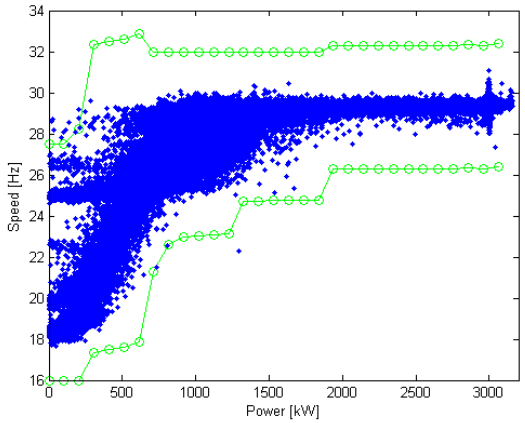

Figure 3. Raw data and dynamic frequency range for initial speed estimation.

3.2. Identification of speed related frequency

The speed related frequency component which serve as fingerprint for the identification of the high speed shaft (generator) running speed shall fulfil two prerequisites:

1. adequate representation within the specified time interval
2. it has to be dominant in the search bandwidth

First and foremost, it is mandatory to specify the rate of update of the running speed (n_{HSS}) estimation. For a geared high speed turbine, where n_{HSS} varies roughly between $17Hz$ to $30Hz$, one shaft revolution corresponds to 0.03 to 0.06 seconds. Bearing in mind that the generator rotor inertia of a multi-megawatt scale turbine is high and that the wind conditions do not change dramatically within 1 second, a fair selection would be to update the speed value every 10 revolutions, namely 0.3 to 0.6 seconds.

The component which has been utilized by the vast majority of researchers is the gearbox high speed stage first tooth mesh frequency ($1TMF$) and its harmonics (Zimroz et al., 2010, 2011). This selection is fully justified based on the following facts. Assuming that the the high speed shaft speed is between $17Hz$ to $30Hz$ and that the high speed stage pinion has 35 teeth, $1TMF$ is approximately between $600Hz$ to $1000Hz$, as shown in 4. This means that in the worst case scenario, at least 180 (=$0.3s \cdot 600Hz$) cycles of the first tooth mesh frequency fit in the specified time interval offering the required representation of the selected frequency component. On the contrary, if the 1^{st} running speed harmonic is used (approximately $17Hz$ to $30Hz$), then only 5 cycles correspond to 0.3 seconds which is considered insufficient.

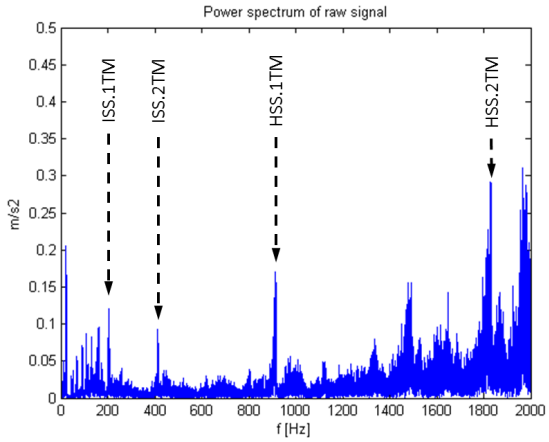

Figure 4. Power spectrum of gearbox High Speed Stage Front Accelerometer. The first two harmonics of the High Speed and Intermediate Speed Stage tooth mesh frequencies are shown by arrows. The objective is to track HSS.1TMF in intervals of 0.3 seconds.

3.3. Validation of results and redundancy

In order to obtain an accurate estimation of the running speed, the result has to be verified so as to eliminate any invalid outcomes which will potentially produce unrealistic trends of the speed related frequencies. Furthermore, the robustness of the method depends on the presence of multiple sources of vibration data where a suitable frequency speed related component can be utilized for the extraction of the actual speed.

Figure 5 illustrates the drive train and the sensor location of a conventional geared turbine. The 3^{rd} stage (also referred as High Speed Stage) of a gearbox is usually monitored by two sensors in order to identify faults on the meshing gears, such as broken teeth and excessive wear, and the bearings supporting the high speed shaft. It should be noted that the sensors installed close to the 2^{nd} stage can be also utilized by detecting the corresponding 1^{st} tooth mesh frequency. The consistency of the results depends highly on the presence of a clear vibration path between the 2^{nd} and 3^{rd} stages' gears and the sensors' location.

4. RUN OF ALGORITHM

In order to have a reliable running speed reconstruction which enhances the capabilities of the condition monitoring system when the speed sensor (tachometer) does not function prop-

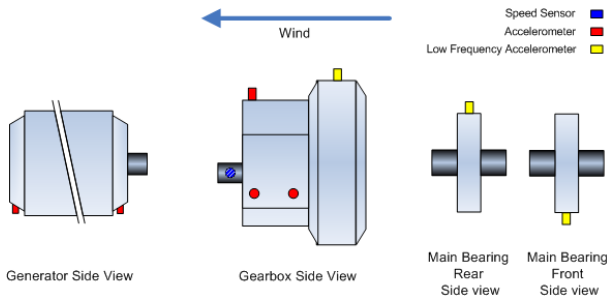

Figure 5. Sensors' location of a typical drive train.

erly, it is required that the applied method and algorithm auto-checks its performance in regular time intervals. It should be born in mind that the estimation of an incorrect speed for a long period of time introduces high uncertainty on the speed related condition indicators rendering the assessment of historic data unreliable.

The installation of two sensors for the high speed stage of the gearbox and the generator bearings offer two sources of vibration data for the extraction of the running speed providing the capability of verifying the method outputs. The basic steps of the proposed speed evaluation techniques are as follows:

1. Verification of invalid signal from speed sensor. This can be achieved by checking the voltage level of the speed signal or detecting unrealistic indications.
2. Loading of gearbox teeth counting.
3. Loading of the dynamic range applicable for each gearbox type, as shown in Fig. 3.
4. Reading of instantaneous power production from the turbine controller and finding the acceptable range.
5. Apply filters to raw time waveforms. This step is executed in order to mitigate the influence of any existing high frequency spectral components.
6. If the algorithm is executed for first time, use wide frequency range to compute the running speed. Otherwise, use previous speed $\pm 0.5Hz$ as valid range.
7. Decision step to accept the estimated speed as valid. There are two conditions: 1) the difference between the estimated speeds from the two accelerometers, ω_{Acc1} and ω_{Acc2} have to be within a specified error; 2) the mean value must be within the dynamic range in step 3. If yes, accept the speed estimation and feed value as reference. In no, check if the speed estimation has been invalid for a maximum number of $0.3s$ intervals. If yes, reset counter and fetch power stamp. If no, use the latest valid speed estimation as reference.

The above described algorithm is displayed in in Figure 6 as flowchart.

In order to illustrate the functionality and robustness of the method, the speed variation is presented in Figure 7 as: 1) recorded from the speed sensor and 2) it is calculated from the High Speed Stage Front ($HssFr$) and High Speed Stage Rear ($HssRr$) accelerometers separately and 3) combining the two vibration sensors. The latter is labelled as "Virtual". It can be seen that the speed values generated when trachting $1TMF$ using the $HssRr$ accelerometer are invalid for $Time > 20s$, which is due to the presence of frequency components around $1TMF$ of comparable amplitude resulting to the occasional collapse of the method on them. If the speed estimation based on the $HssRr$ accelerometer is taken into account, then the uncertainty regarding the correct value will be high. Therefore, this case shows the advantage of having two sources for the reconstruction of the speed signal and how temporary effects affect the tracking of the maximum correlation coefficient.

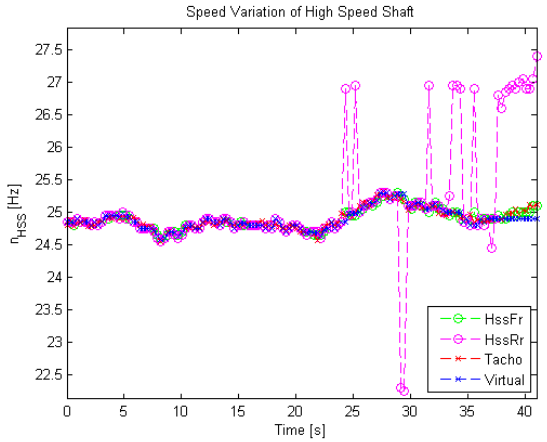

Figure 7. Estimated speed variation based on gearbox 3^{rd} stage accelerometers. Although one of the vibration sensors generates invalid results for the second half of the file, the algorithm performs an auto-check and keeps the latest valid speed estimation. It can be observed that the virtual speed for the last few seconds is kept stable at the latest valid result. If this condition continues for a predefined period then a full scan of the wide frequency range takes place. The accuracy is set to be $0.05Hz$.

An important aspect is the performance of the method under large speed fluctuations. Figure 8 shows a case where the speed variation is 14.27% or $3.65Hz$ ($219rpm$). In more details the turbine accelerates during the first $6.65s$ and slowly decelerates giving a variation of $33rpm/s$ for the first portion.

5. VALIDATION OF SPEED ESTIMATION METHOD

The method described in section 2.1 is tested in three drive train configurations where the number of main bearings and gearbox layout are different. The three topologies are:

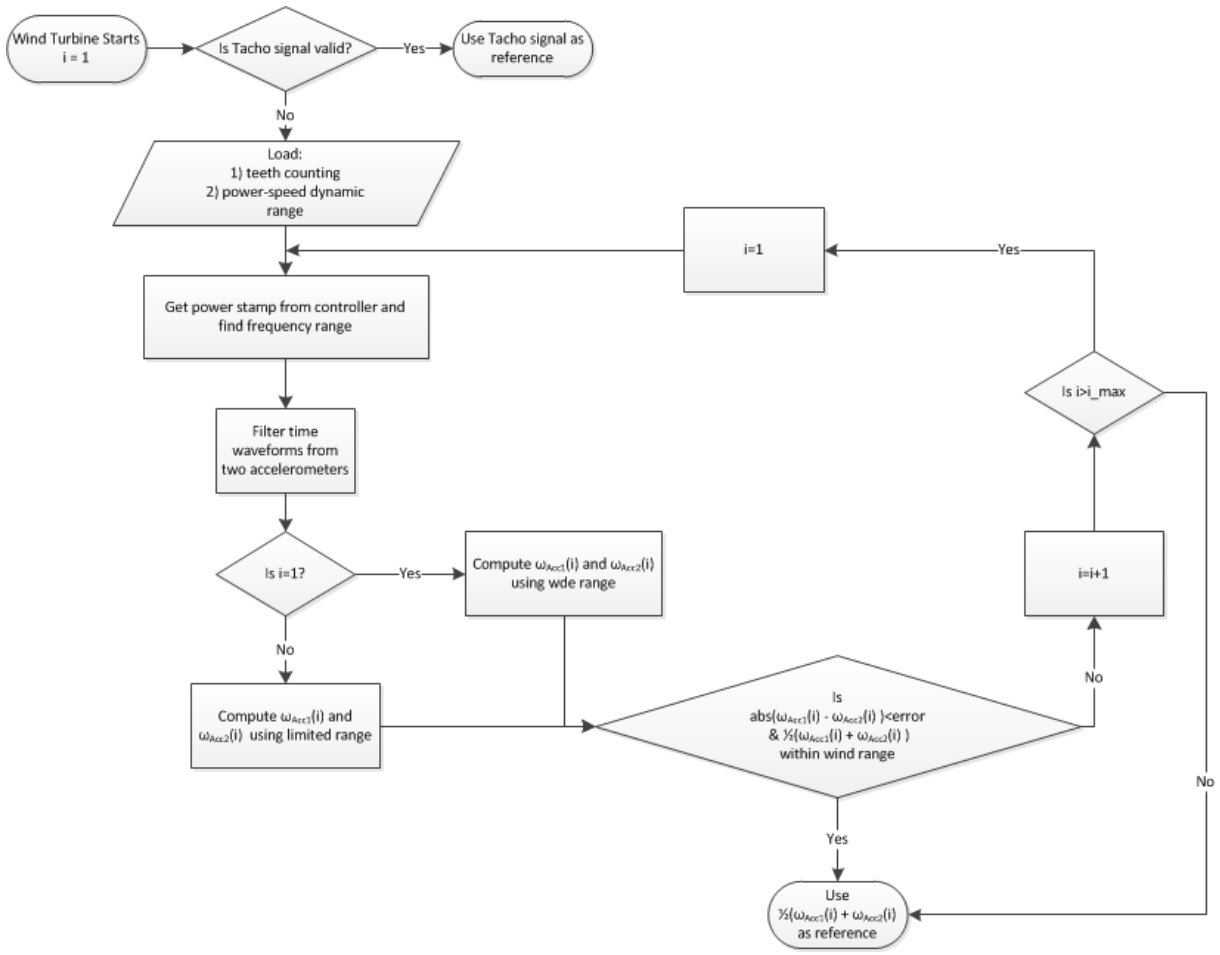

Figure 6. Flowchart showing the basic steps of the proposed speed evaluation algorithm.

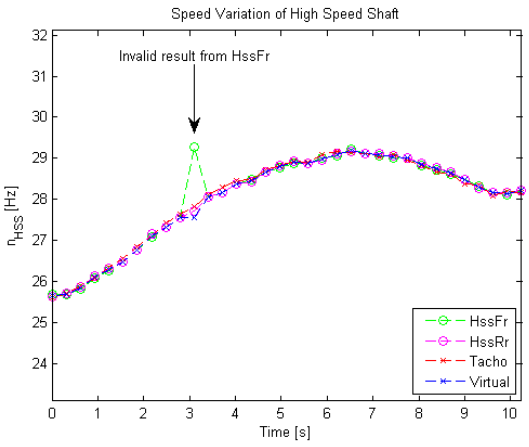

Figure 8. Estimated speed variation based on gearbox 3^{rd} stage accelerometers. The accuracy is set to be $0.05Hz$ and the time interval between two estimation is $0.3s$.

1. Two main bearings, three stage gearbox (one planetary and two helical – 1P2H)
2. One main bearing, three stage gearbox (two planetary and one helical – 2P1H)
3. One main bearing, four stage gearbox (three planetary and one helical –3P1H)

The speed estimation algorithm is tested in 40 turbines per topology installed worldwide – 120 turbines in total. Six 10.24 second gearbox or generator vibration signals sampled at 25.6kHz are analyzed for each turbine. The time interval between two consecutive files is approximately two days, offering the possibility of investigating the efficiency of the method at different wind conditions. Furthermore, the aforementioned 120 turbines fulfil two conditions: 1) the actual speed signal is valid for comparison purposes and 2) the signals generated by the accelerometers mounted on the gearbox are valid.

The random selection of turbines ensures that the method is independent of the rotor diameter, turbine wind class and con-

troller settings as long as the same gearbox is installed on them. The illustrated figures in the following sections consist of three bars; the first two bars present the cases where only one source of vibration data is used, whereas the third bar corresponds to the combined utilization of two sensors and it serves as indicator of the robustness of the method. The acceptable error limit is selected to be 0.25Hz throughout the following analysis.

5.1. First topology – Three stage gearbox (1P2H)

The first gearbox layout consists of one slow rotating planetary and two helical stages. The utilized vibration signals are recorded by two accelerometers mounted on strategically selected positions adjacent to the high speed stage bearing housings in order to achieve optimum vibration path.

The used abbreviations in the following figures are HssFr (High Speed Stage Front), HssRr (High Speed Stage Rear) and Fr-Rr suggesting that the response of both accelerometers is accounted. It can be observed that although the success rate is above 90%, the percentage of valid estimations is relatively lower when only the High Speed Stage Front accelerometer is used. This behaviour is assessed to be linked to the presence of a mechanically driven oil pump located close to this sensor introducing high noise interference around the high speed stage 1TMF. Of course, the vibration signal from the High Speed Stage Rear sensor suffers also from noise but the influence is limited.

The invalid outcomes of the third column in Fig. 9 count for 1.25% of the test set which suggests that the algorithm yields incorrect estimations for 9 out of 720 files. The latter can be translated as that for the considered 10.24s, a frequency component close to the 1TMF is of higher amplitude and therefore the method collapses to this maximum. However, it should be underlined that the invalid results are not originated by the same turbine implying that temporary local phenomena influence the speed estimation.

Figures 10 and 11 shows the maximum absolute error distributions as function of the mean power production and the speed variation within 10.24s for the two sensors. The following remarks can be made:

- the method generates valid estimations even in the extreme cases where the speed variation is approximately 11% (approximately 300rpm) rendering it robust to large speed changes.
- the HssRr sensor presents less incorrect estimations in the high power range which is most likely associated with the operation and influence of the oil pump.
- the maximum absolute difference, when only the High Speed Stage Front is used, is approximately identical for all the incorrect estimations. This is again assessed to be directly linked to the oil pump operation.

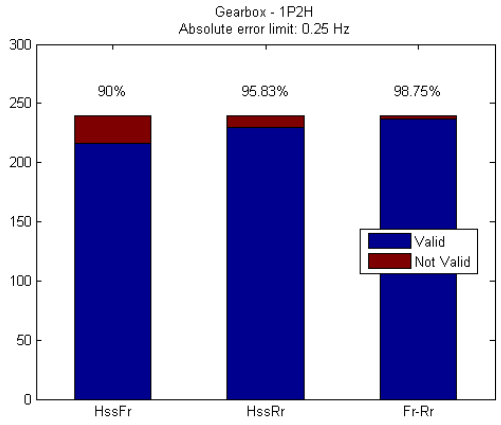

Figure 9. Validation of speed estimation for the 1^{st} topology based on mean square error.

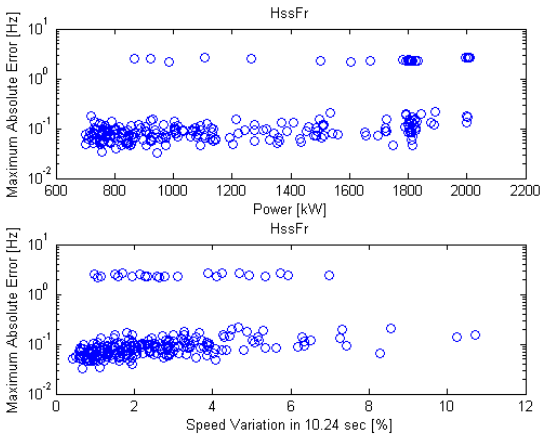

Figure 10. 1^{st} topology - Maximum absolute error from 120 files as function of the mean power production and speed variation in 10.24s - High speed stage front (HssFr) sensor.

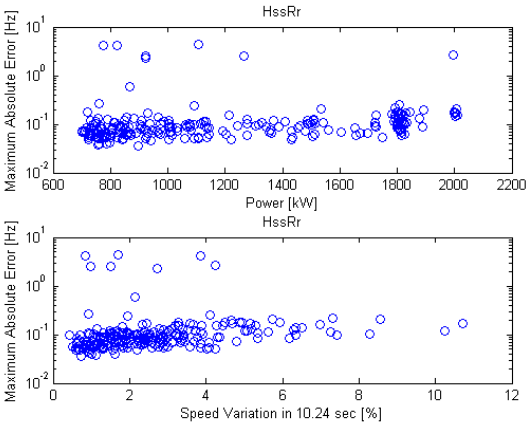

Figure 11. 1^{st} topology - Maximum absolute error from 120 files as function of the mean power production and speed variation in 10.24s - High speed stage rear (HssRr) sensor.

5.2. Second topology – Three stage gearbox (2P1H)

The high speed stage of the second topology (two planetary and one helical stages) is also monitored by two sensors mounted adjacent to the high speed stage support bearings offering the capability of validating the speed estimation from two vibration sources. Fig. 12 presents the results for the error limits under examination. It is observed that the certainty level that at least one sensor yields consistent speed estimation approaches is in the range between 90 to 100%. The main sources of interference which have resulted to invalid results for this gearbox type are:

- increased sideband activity due to misaligned/eccentric gears, issues such as macropitting, stand-still marks, cracked and broken teeth or bearing defects (located mainly at the inner race)
- low amplitude of the 1TMF, which is assessed to be related to the vibration signature of the gearbox and not to a specific failure mode

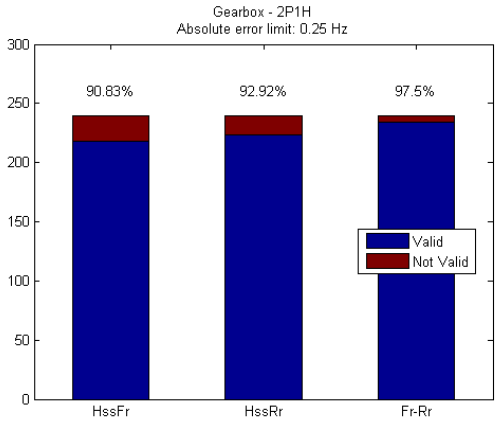

Figure 12. Validation of speed estimation for the 2^{nd} topology based on absolute error.

As in the first topology, the speed estimation algorithm generates reliable results for both low and high speed variations. Furthermore, no straight correlation was observed between the power production and the number of invalid results fact, showing that any mismatches are random.

5.3. Third topology – Four stage gearbox (3P1H)

The third gearbox topology consists of four stages in total, three planetary and one helical. The maximum absolute errors generated by the two accelerometers monitoring the high speed stage are presented in Figure 13. The third bar shows the results when both vibration sensors are used to cross-reference the speed estimation; it is reminded that the third bar presents the certainty level that the algorithm can identify a correct or incorrect result.

The following observations can be made:

- the speed estimations from the HssFr sensor are considerably poorer compared to the HssRr one, which is assessed to be related to the construction of the gearbox and location of the sensor. For this gearbox, a clear vibration path applies not only from the helical stage to the sensor but also from the last planetary stage to it.
- although the speed estimation success rate from each sensor individually is low, the valid results when both are accounted are acceptable. This implies that only for approximately $3-4\%$ of the files the algorithm regards an invalid result as valid.

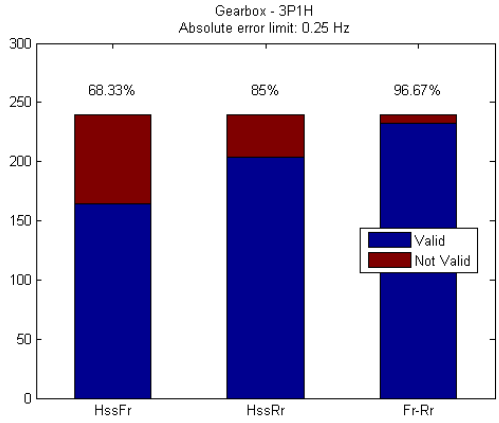

Figure 13. Validation of speed estimation for the 3^{rd} topology using the high speed stage gearbox vibration sensors based on absolute error.

6. CONCLUSIONS

The present paper presents the application of the maximum correlation coefficient on the estimation of the high speed shaft speed utilizing two sources of vibration data for validation and cross referencing purposes. Three drive train topologies and gearbox layouts are studied in this work, where 720 files in total serve as test sample. Statistical analysis reveals that the technique offers reliable results for more than 98% of the cases when the performed analysis is based on two accelerometers. The success rate is lower, close to 90%, when the speed estimation algorithm input is only one vibration signal, emphasizing the necessity of validating the outcome. In specific, in one of the gearbox configurations, the presence of auxiliary equipment, i.e. a mechanically driven oil pump, influences the speed estimation performance based on the accelerometer located closer to it. In the third topology, the presence of strong vibration path between one of the accelerometer under consideration and more than one gearbox stages, results in incorrect speed estimations for approximately 30% of the cases, which again supports the employment of two vibration sources. Finally, it has not been ob-

served any direct dependency between the algorithm's efficiency and large speed variations or power output dependency, rendering the method robust.

REFERENCES

Andersson, C., Gutt, S., & Hastings, M. (2007). Cost–effective monitoring solution using external surveillance centre. In *The 2nd world congress on engineering asset management (eam) and the 4th international conference on condition monitoring.*

Bartelmus, W., & Zimroz, R. (2009). Vibration condition monitoring of planetary gearbox under varying external load. *Mechanical Systems and Signal Processing*, *23*, 246–257.

Bellini, A., Franceschini, G., & Tassoni, C. (2006). Monitoring of induction machines by maximum covariance method for frequency tracking. *Industry Applications , IEEE Transactions on*, *42*(1), 69–78.

Bonnardot, F., Badaloui, M. E., Randall, R. B., Danie're, J., & Guillet, F. (2005). Use of the acceleration signal of a gearbox in order to perform angular resampling (with limited speed fluctuation). *Mechanical Systems and Signal Processing*, *19*, 766 – 785.

Borghesani, P., Pennacchi, P., Randall, R., & Ricci, R. (2012). Order tracking for discrete-random separation in variable speed conditions. *Mechanical Systems and Signal Processing*, *30*, 1 – 22.

Coats, M. D., Sawalhi, N., & Randall, R. (2009). Extraction of tach information from a vibration signal for improved synchronous averaging. In *Proceedings of acoustics.*

Combet, F., & Zimroz;, R. (2009). A new method for the estimation of the instantaneous speed relative fluctuation in a vibration signal based on the short time scale transform. *Mechanical Systems and Signal Processing*, *23*, 1382 – 1397.

Marhadi, K., & Hilmisson, R. (2013, June). Simple and effective technique for early detection of rolling element bearing fault: A case study in wind turbine application. In *International congress of condition monitoring and diagnostic engineering management* (pp. 94–97).

Peng, Z., Meng, G., Chu, F., Lang, Z., Zhang, W., & Yang, Y. (2011). Polynomial chirplet transform with application to instantaneous frequency estimation. *Instrumentation and Measurement, IEEE Transactions on*, *60*(9), 3222 – 3229.

Taylor, J. I. (2000). *The gear analysis handbook* (VIBRATIONS-WILLOWBROOK, Ed.). The Vibration Institute.

Urbanek, J., Zimroz, R., Barszcz, T., & Antoni, J. (n.d.). Reconstruction of rotational speed from vibration signal – comparison of methods. In *The ninth conference on condition monitoring and machine failure prevention technologies.*

Villa, L. F., Reñones, A., Perán, J. R., & De Miguel, L. J. (2011). Angular resampling for vibration analysis in wind turbines under non-linear speed fluctuation. *Mechanical Systems and Signal Processing*, *25*(6), 2157 – 2168.

Wu, W., Lin, J., Han, S., & Ding, X. (2009). Time domain averaging based on fractional delay filter. *Mechanical Systems and Signal Processing*, *23*, 1447–1457.

Yiakopoulos, C., Gryllias, K., & Antoniadis, I. (2009). Instantaneous frequency in rotating machinery using harmonic signal decomposition (hard) parametric method. In *Proceedings of the asme international design engineering conference and computers and irnformation in engineering conference* (pp. 1205 – 1213).

Zhao, M., Lin, J., Wang, X., Lei, Y., & Cao, J. (2013). A tacho-less order tracking technique for large speed variations. *Mechanical Systems and Signal Processing*, *40*, 76 – 90.

Zimroz, R., Millioz, F., Martin, N., et al. (2010). A procedure of vibration analysis from planetary gearbox under non-stationary cyclic operations by instantaneous frequency estimation in time-frequency domain. In *Seventh international conference on condition monitoring and machinery failure prevention technologies. cm 2010 and mfpt 2010.*

Zimroz, R., Urbanek, J., Barszcz, T., Bartelmus, W., Millioz, F., & Martin, N. (2011). Measurement of instantaneous shaft speed by advanced vibration signal processing-application to wind turbine gearbox. *Metrology and Measurement Systems*, *18*(4), 701 – 712.

BIOGRAPHIES

Georgios Alexandros Skrimpas received the Diploma in electrical and computer engineering from the Aristotle University of Thessaloniki, Greece, in 2009 and the M. Sc. in wind energy from the Technical University of Denmark (DTU) in 2012. He joined Brüel and Kjær Vibro in 2012 and since 2013 he is pursuing the Industrial Ph.D. degree at the Centre of Electric Power and Energy at DTU in cooperation with Brüel and Kjær Vibro. His research interests are diagnosis and prognosis of electrical and mechanical faults in wind turbines.

Kun S. Marhadi is an engineer in the Remote Monitoring Group at Brüel and Kjær Vibro. He joined Brüel and Kjær Vibro in 2012. Previously, he worked as a postdoctoral fellow in the Department of Mathematics at the Technical University of Denmark (DTU). He received his PhD in computational science in 2010 from San Diego State University and Claremont Graduate University. He has M.S. and B.S. in aerospace engineering from Texas A&M University. His expertise is in structural vibration and analyses, probabilistic methods, and design optimization.

Bogi Bech Jensen received the Ph.D. degree from Newcastle University, Newcastle Upon Tyne, U.K., for his work on induction machine design. He was in various engineering and academic positions in the marine sector from 1994 to 2004.

He was at Newcastle University from 2004 to 2010 first as a Postgraduate, then Research Associate and finally as a Lecturer. From 2010 to 2014 he was Associate Professor and later Head of Research Group at the Technical University of Denmark (DTU), Lyngby, Denmark. He is currently Professor of Energy Engineering at the University of the Faroe Islands (UFI), where he is responsible for education and research in energy. Prof. Jensen is Associate Editor of IEEE Transactions on Industry Applications and a Senior Member of IEEE.

Christian Walsted Sweeney received his B.Sc. degree from the University of Southern Denmark in 2006 and M.Sc degree from the Technical University of Denmark in 2008 both in mechanical engineering. From 2008 to 2010 he was employed by Brüel and Kjær Vibro as diagnostic engineer and since 2010 he is the team leader of the diagnostic services group. His research focus is on the development of condition monitoring systems and handling of large data quantities.

Nenad Mijatovic received his Ph.D. degree from the Technical University of Denmark for his work in superconducting machine. After obtainnign his Dipl.Ing. education at University of Belgrade, Serbia, he enrolled as a doctoral candidate in 2012. Upon completion of the PhD, he has continued to work in the same field of machine research - superconducting machines, as an Industrial PostDoc. The 3 year industrial PostDoc grant has been provided by Hojteknologifonden and supported by Envision Energy Aps., Denmark. Dr. N. Mijatovic is a member of IEEE from 2008 and his field of interest and research includes novel electrical machine design, operations and diagnostic.

Joachim Holboell is associate professor and deputy head of center at DTU, Department of Electrical Engineering, Center for Electric Power and Energy. His main field of research is high voltage components, their properties, condition and broad band performance, including insulation systems performance under AC, DC and transients. Focus is also on wind turbine technology and future power grid applications of components. J. Holboell is Senior Member of IEEE.